

COMPARATIVE THERMODYNAMIC STUDY AND CHARACTERIZATION OF TERNARY Ag–In–Sn ALLOYS

Dragana Živković^{1*}, A. Milosavljević², A. Mitovski¹ and B. Marjanović¹

¹University of Belgrade, Technical Faculty, VJ 12, 19210 Bor, Serbia

²Copper Institute, Zeleni bulevar bb, 19210 Bor, Serbia

The results of thermodynamics and characterization of alloys in ternary Ag–In–Sn system is presented in this paper. Thermodynamic properties, in three investigated sections with molar ratio In:Sn=1:1, 1:2 and 1:4, have been calculated at the temperature of 1423 K using different predicting methods (general solution model, Toop, Hillert, Muggianu, Kohler, Redlich-Kister), compared mutually and with literature experimental data. The alloys in investigated sections have been characterized using DTA, XRD, SEM and optical microscopy.

Keywords: Ag–In–Sn system, alloys, characterization, lead-free solders, thermodynamics

Introduction

One among different lead-free solder candidates is the Ag–In–Sn system [1]. Due to its expected application, numerous investigations have been done recently in order to determine the most important characteristics of this system [2–8], including mostly phase equilibria considerations and thermodynamic analysis. Optimized thermodynamic data for constitutive binary systems may be found in COST 531 Database [9].

Thermodynamic investigations of the Ag–In–Sn system started with the work of Gather *et al.* [2], who determined the enthalpies of mixing in the liquid state for four sections in the Ag–In–Sn system using a heat flow calorimeter. Miki *et al.* [3] studied the activities of the constituents in the Ag–In–Sn system experimentally, using a mass spectrometry and performing the measurements in the temperature range 1273–1523 K. Zhang [4] calculated a model of mass action concentration for metallic Ag–In–Sn melts and compared its results with measured activities at 1423 K.

In the frame of phase diagram determination, Korhonen and Kivilahti [5] have studied ternary alloys at 523 K using DSC, X-ray, SEM and metallography. Liu *et al.* [6] gave an important contribution on experimental determination and thermodynamic calculation of the phase equilibria in the Ag–In–Sn system, based on the DSC and metallographic results performed. The most recent reference is the work of Vassilev *et al.* [7], who did an experimental study of the Ag–In–Sn diagram at 553 K using DSC, X-ray and SEM and determined the solubility ranges of the solid solution and the intermetallic phases. Also, an isothermal phase diagram of the

Ag–In–Sn system at 386 K, together with microsegregation in the Sn₂₀In_{2.8}Ag solder alloys, may be found in [8].

As a contribution to the more complete knowledge of the Ag–In–Sn system thermodynamics and structural characteristics, the results of thermodynamic investigation and characterization of alloys in ternary Ag–In–Sn system is presented in this paper. Thermodynamic properties, in two investigated sections with molar ratio In:Sn=1:1, 1:2 and 1:4, have been calculated using different predicting methods (Redlich-Kister, general solution model, Toop, Hillert, Muggianu, Kohler) and compared.

Theoretical fundamentals

Calculation of thermodynamic properties for the Ag–In–Sn alloys in three investigated sections with molar ratio In:Sn=1:1, 1:2 and 1:4, have been done using different predicting methods – general solution model [10, 11], Toop [12], Hillert [13], Muggianu [14], Kohler [15], and Redlich-Kister model [16].

The basic equations of used models are given as follows:

General solution model [10, 11]

$$\begin{aligned}
 G^E = & x_1x_2(L_{12}^0 + A_{12}^1(x_1-x_2) + A_{12}^2(x_1-x_2)^2) + \\
 & + x_2x_3(A_{23}^0 + A_{23}^1(x_2-x_3) + A_{23}^2(x_2-x_3)^2) + \\
 & + x_3x_1(A_{31}^0 + A_{31}^1(x_3-x_1) + A_{31}^2(x_3-x_1)^2) + fx_1x_2x_3
 \end{aligned} \quad (1)$$

* Author for correspondence: dzivkovic@tf.bor.ac.yu

where A_{ij}^0 , A_{ij}^1 , A_{ij}^2 are parameters for binary system 'ij' independent of composition, only relying on temperature, which have been used in the regular type equation:

$$\Delta G_{ij}^E = X_i X_j (A_{ij}^0 + A_{ij}^1 (X_i - X_j) + A_{ij}^2 (X_i - X_j)^2 + \dots + A_{ij}^n (X_i - X_j)^n) \quad (2)$$

where X_i and X_j indicate the mole fraction of component 'i' and 'j' in 'ij' binary system. The function f is the ternary interaction coefficient expressed by:

$$f = (2\xi_{12} - 1) \{ A_{12}^2 ((2\xi_{12} - 1)x_3 + 2(x_1 - x_2)) + A_{12}^1 \} + (2\xi_{23} - 1) \{ A_{23}^2 ((2\xi_{23} - 1)x_1 + 2(x_2 - x_3)) + A_{23}^1 \} + (2\xi_{31} - 1) \{ A_{31}^2 ((2\xi_{31} - 1)x_2 + 2(x_3 - x_1)) + A_{31}^1 \} \quad (3)$$

where ξ_{ij} are the similarity coefficients defined by η_i called the deviation sum of squares:

$$\xi_{ij} = \eta_i / (\eta_i + \eta_j) \quad (4)$$

where

$$\eta_I = \int_{X_i=0}^{X_i=1} (\Delta G_{12}^E - \Delta G_{13}^E)^2 dX_1$$

$$\eta_{II} = \int_{X_i=0}^{X_i=1} (\Delta G_{21}^E - \Delta G_{23}^E)^2 dX_2$$

$$\eta_{III} = \int_{X_i=0}^{X_i=1} (\Delta G_{31}^E - \Delta G_{32}^E)^2 dX_3 \quad (5)$$

and

$$X_{1(12)} = x_1 + x_3 \xi_{12}$$

$$X_{2(23)} = x_2 + x_1 \xi_{23} \quad (6)$$

$$X_{3(31)} = x_3 + x_2 \xi_{31}$$

Toop model [12]

$$G^E = \frac{x_2}{1-x_1} \Delta G_{12}^E(x_1; 1-x_1) + \frac{x_3}{1-x_1} \Delta G_{13}^E(x_1; 1-x) + (x_2 + x_3)^2 \Delta G_{23}^E \left(\frac{x_2}{x_2 + x_3}; \frac{x_3}{x_2 + x_3} \right) \quad (7)$$

Hillert model [13]

$$G^E = \frac{x_2}{1-x_1} \Delta G_{12}^E(x_1; 1-x_1) + \frac{x_3}{1-x_1} \Delta G_{13}^E(x_1; 1-x_1) + \frac{x_2 x_3}{v_{23} v_{32}} \Delta G_{23}^E(v_{23}; v_{32}) \quad (8)$$

where: $v_{ij} = 1/2(1+x_i-x_j)$

Muggianu model [14]

$$G^E = \frac{4x_1 x_2}{(1-x_1-x_2)(1+x_2-x_1)} \Delta G_{12}^E \left(\frac{1+x_1-x_2}{2}; \frac{1+x_2-x_1}{2} \right) + \frac{4x_2 x_3}{(1+x_2-x_3)(1+x_3-x_2)} \Delta G_{23}^E \left(\frac{1+x_2-x_3}{2}; \frac{1+x_3-x_2}{2} \right) + \frac{4x_3 x_1}{(1+x_3-x_1)(1+x_1-x_3)} \Delta G_{31}^E \left(\frac{1+x_3-x_1}{2}; \frac{1+x_1-x_3}{2} \right) \quad (9)$$

Kohler model [15]

$$G^E = (x_1 + x_2)^2 \Delta G_{12}^E \left(\frac{x_1}{x_1 + x_2}; \frac{x_2}{x_1 + x_2} \right) + (x_2 + x_3)^2 \Delta G_{23}^E \left(\frac{x_2}{x_2 + x_3}; \frac{x_3}{x_2 + x_3} \right) + (x_3 + x_1)^2 \Delta G_{31}^E \left(\frac{x_3}{x_1 + x_3}; \frac{x_1}{x_1 + x_3} \right) \quad (10)$$

Redlich-Kister model [16]

$$G^E = x_1 x_2 [L_{12}^0 + (x_1 - x_2)L_{12}^1 + (x_1 - x_2)^2 L_{12}^2 + \dots] + x_2 x_3 [L_{23}^0 + (x_2 - x_3)L_{23}^1 + (x_2 - x_3)^2 L_{23}^2 + \dots] + x_1 x_3 [L_{13}^0 + (x_1 - x_3)L_{13}^1 + (x_1 - x_3)^2 L_{13}^2 + \dots] + x_1 x_2 x_3 f_{123} \quad (11)$$

where f_{123} presents the ternary interaction parameter, usually expressed in the form: $f_{123} = x_1 L_{123}^0 + x_2 L_{123}^1 + x_3 L_{123}^2$, with a temperature dependence taken as $L_{123}^v = a^v + b^v T$ ($v=0, 1, 2$).

In all given equations, G^E and ΔG_{ij}^E correspond to the integral molar excess Gibbs energies for ternary and binary systems, respectively, while x_1, x_2, x_3 correspond to the mole fraction of components in investigated ternary system.

Experimental

Experimental investigations presented in this paper were done using differential thermal analysis (DTA), X-ray diffraction analysis (XRD), scanning electron microscopy (SEM) and optic microscopy.

DTA analysis was done on derivatograph MOM, Budapest (Hungary), at the heating rate of 10 K min⁻¹ in an air atmosphere, while Al₂O₃ was used as a referent material during measurements.

XRD analysis was performed on Siemens apparatus, using Cu-anticathode and Ni-filters (40 kV, 20 mA).

SEM analysis was performed on JEOL-JSM T20 scanning microscope. Solution (32g FeCl₃+100 mL H₂O₂+100 mL H₂O) was used as the etching agents for the samples prepared according to the standard metallographic procedure.

Microstructure analysis of the investigated samples was examined by optic microscopy, using a Reichert MeF2 microscope.

All experiments were carried out in an air atmosphere, with Ag, In and Sn metals of p.a. purity. Samples–alloys with mole content of silver equal to 0.1, 0.2, 0.3, 0.4 and 0.5 in the section with molar ratio In:Sn=1:1 have been experimentally investigated.

Results and discussion

Basic data for the calculation were the values of integral molar Gibbs excess energies, ΔG_{ij}^E , for the constitutive binary systems Ag–In, In–Sn and Sn–Ag taken from Moser *et al.* [17], Lee *et al.* [18] and Oh *et al.* [19], respectively (according to COST 531 database [9]). The Redlich-Kister parameters (which also correspond to the parameters A_{ij}^n in Eqs (1), (2) for the liquid phase of constituting binaries in the temperature range, are given in Table 1, together with the Redlich-Kister parameters of the liquid phase of ternary Ag–In–Sn system, taken from [6].

Further, for the purpose of calculation according to the general solution model, related similarity coefficients were determined using Eq. (4) at the investigated temperature of 1423 K. Their values are as follows: $\xi_{AgIn}=0.268$, $\xi_{InSn}=0.871$ and $\xi_{SnAg}=0.288$. Graphical presentation of the selected binary compositions for three constitutive binaries in the Ag–In–Sn system at the temperature of 1423 K, is shown in Fig. 1.

The values of integral molar Gibbs excess energies for the alloys in investigated sections in ternary Ag–In–Sn system were calculated using general solution model (GSM), Redlich-Kister (RKM), Toop, Hillert, Kohler and Muggianu models. The comparative graphical presentation with literature experimental data [3] at 1423 K is shown in Fig. 2.

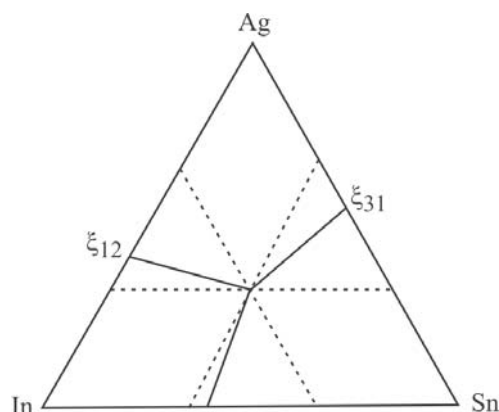


Fig. 1 The selected binary compositions for three binaries in the ternary system Ag–In–Sn according to general solution model at 1423 K (shown as bold solid lines)

As can be seen in Fig. 2, there are differences between applied predicting models, especially between the asymmetric and symmetric models. Also, there are differences between different models and experimental literature data [3], while best agreement may be noticed for asymmetric models – Toop and Hillert. The results of Redlich-Kister model application, using ternary interaction parameter taken from [6], show agreement with experiments over the composition of $x_{Ag}=0.6$, but significant deviation for lower silver concentrations.

In order to determine accurately the most adequate thermodynamic model for liquid Ag–In–Sn alloys among used ones, the root mean square deviation analysis was applied on GE data obtained for mentioned three sections:

$$RMS = 1/N[\sum(G_{exp}^E - G_{calc}^E)^2]^{1/2} \quad (12)$$

where: RMS – root mean square deviation, N – the number of counting points, G_{exp}^E – experimental, literature results [3] for G^E and G_{calc}^E – calculated values for G^E . The results of such analysis, applied to all investigated sections, are presented in Table 2.

Taking into account Figs 1, 2 and Table 2, it is obvious that investigated Ag–In–Sn system could be regarded as an asymmetric system and according to the root mean square analysis, the Toop model is adequate model for thermodynamic description of liquid Ag–In–Sn alloys.

Table 1 Redlich-Kister parameters for the liquid phase of constitutive binaries

System	$L^0(T)$	$L^1(T)$	$L^2(T)$	$L^3(T)$
Ag–In	$-14403.297-8.176T$	$-15551.028-2.664T$	$-710.629-5.293T$	3955.27
In–Sn	-828.54	$0.76018-0.1211767T\log T$	0	0
Ag–Sn	$-5146.7-5.0103T$	$-15799.3+3.3208T$	-6687.5	0
Ag–In–Sn	$64697-8.82T$	$23474-22.792T$	$13374-27.171T$	0

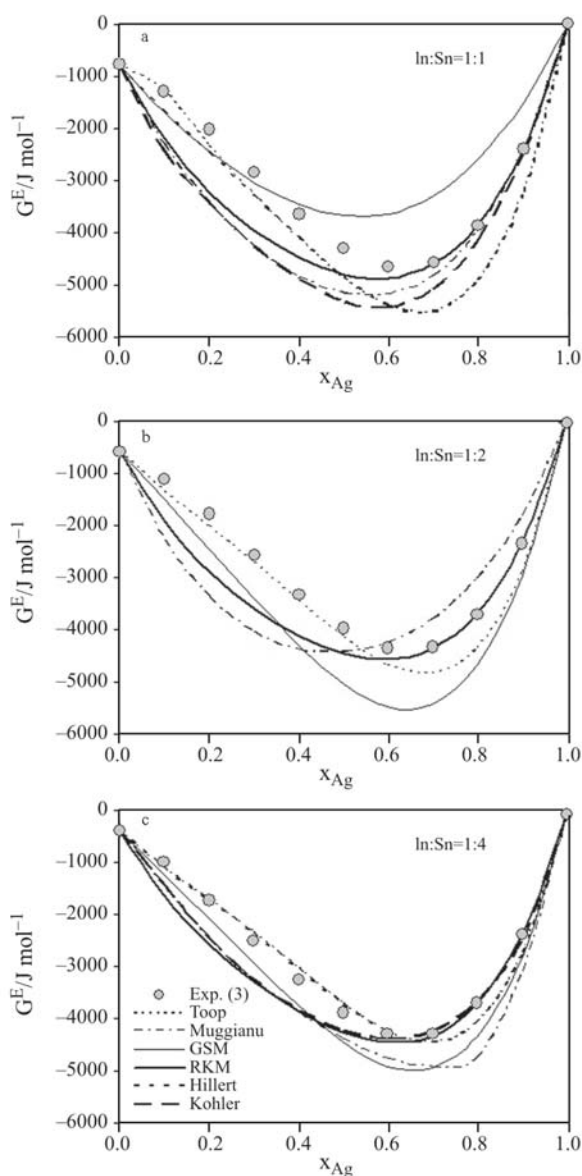


Fig. 2 Comparison of calculated results for G^E with literature experimental data [3] at 1423 K a – In:Sn=1:1; b – In:Sn=1:2; c – In:Sn=1:4

For that reason, further calculation of silver activities in ternary Ag–In–Sn system was done using the Toop model, as well as by the Redlich-Kister model using ternary thermodynamic parameters presented in [6]. As an illustration of the obtained data, characteristic dependence of silver activities on composition, compared with literature data, is shown in Fig. 3 for the section with molar ratio In:Sn=1:1 at 1423 K.

The dependence shown in Fig. 3 confirms that better agreement with experiments [3] was obtained

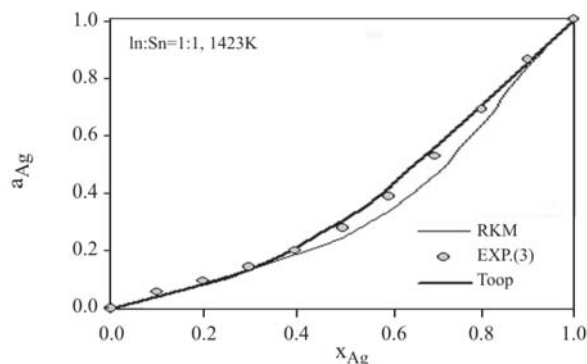


Fig. 3 Comparison of calculated and experimental data [3] for silver activities in investigated Ag–In–Sn system at 1423 K

by Toop model instead of Redlich-Kister model application. Therefore, it may be concluded that introduction of ternary interaction parameter [6] had no specific influence on thermodynamic properties of the Ag–In–Sn system.

Besides thermodynamic study, the alloys in the section with molar ratio In:Sn=1:1 have been experimentally investigated and characterized by means of DTA, XRD, SEM and optic microscopy.

The temperatures of characteristic endothermic effects, obtained by DTA measurements for the concentration part up to $x_{Ag}=0.5$ in the temperature range up to 773 K, are presented in Fig. 4. These values are in accordance with the temperatures of calculated invariant reactions in [6], occurring in the investigated part of the Ag–In–Sn system.

The results of XRD, including identified phases in the samples with molar content of silver equal to 0.1, 0.2 and 0.4 are presented in Table 3, while typical diffractogram for the alloy with $x_{Ag}=0.2$ is shown in Fig. 5.

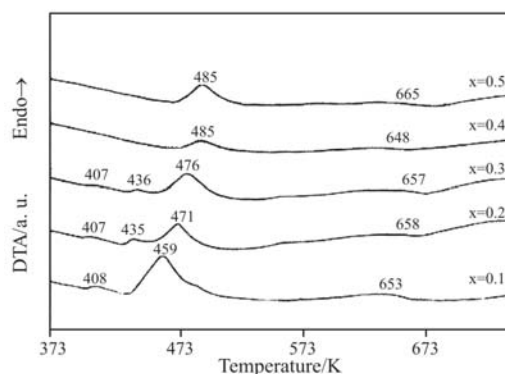


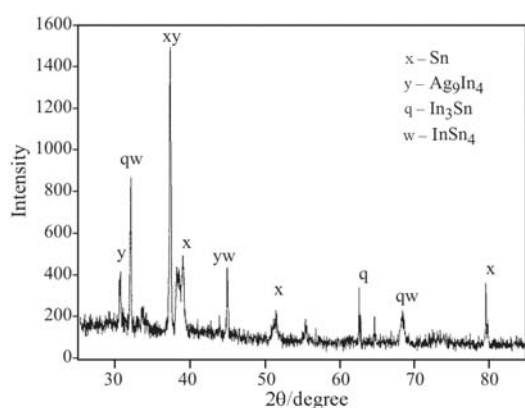
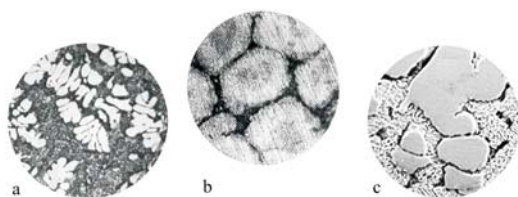
Fig. 4 DTA curves for the investigated alloys with compositions up to $x_{Ag}=0.5$; In:Sn=1:1

Table 2 The root mean square (RMS) deviation to experimental data for each calculation model

Model	GSM	RKM	Toop	Hillert	Kohler	Muggianu
RMS/J mol ⁻¹	126.72	104.82	76.63	78.88	147.51	145.13

Table 3 Phases identified XRD results of the investigated samples

xAg	xIn	xSn	Identified phases				
			Sn	InSn ₄	In ₃ Sn	Ag ₉ In ₄	AgIn
0.1	0.45	0.45	+		+	+	+
0.2	0.4	0.4	+	+	+	+	
0.4	0.3	0.3	+	+		+	+

**Fig. 5** Diffractogram of the Ag₆₀In₂₀Sn₂₀ alloy**Fig. 6** The results of optic microscopy (a, b) and SEM analysis (c) of the investigated Ag–In–Sn alloys
a – Ag₁₀In₄₅Sn₄₅ – ×310; b – Ag₄₀In₃₀Sn₃₀ – ×500;
c – Ag₁₀In₄₅Sn₄₅ – ×1000

The identification was done only using available ASTM reflections for the constituent metals and binary systems in the ternary Ag–In–Sn system [20]. Therefore, obtained results could be partially used for the determination of the investigated alloys composition, because some unidentified peaks in the recorded diffractograms are probably due to the possible existence of some ternary phases occurring in the system.

The results of optic microscopy and SEM analysis for the Ag–In–Sn alloys with molar content equal to 0.1 and 0.4, are presented in Fig. 6.

Microstructure analysis of the investigated samples shows structure, consisting of light – ξ (hcp) Ag–In based phase and dark phase – liquid. Such obtained results are in accordance with the calculated phase diagrams of the vertical sections in the Ag–In–Sn system [6].

Conclusions

The results of comparative thermodynamic study of the Ag–In–Sn alloys, obtained using different predicting models, point out to asymmetric behaviour of investigated system. The Toop model has been determined as most accurate calculating method, comparing to literature experimental data [3]. Also, it was shown that introduction of ternary interaction parameter [6] had no specific influence on thermodynamic properties of the Ag–In–Sn system. Future investigation of this system will be interesting from the experimental thermodynamic point of view, using some of calorimetric techniques [21, 22].

Characterization of some Ag–In–Sn alloys enabled determination of the temperatures of characteristic endothermic effects using DTA, as well as identification of present phases in chosen samples using XRD. These results have been completed using optic microscopy and SEM analysis.

Acknowledgements

The first author is grateful to the Ministry of Science and Environmental Protection of the Republic of Serbia (Project No. 142043) for financial support.

References

- 1 <http://www.ap.univie.ac.at/users/www.cost531>
- 2 B. Gather, P. Schroter and R. Blachnik, *Z. Metallknd.*, 78 (1987) 280.
- 3 T. Miki, N. Ogawa, T. Nagasaka and M. Hino, *Mater. Trans. JIM*, 42 (2001) 732.
- 4 J. Zhang, *Calphad*, 27 (2003) 9.
- 5 T. M. Korhonen and J. K. Kivilahti, *J. Electron. Mater.*, 27 (1998) 149.
- 6 X. J. Liu, Y. Inohana, Y. Takaku, I. Ohnuma, R. Kainuma, K. Ishida, Z. Moser, W. Gasior and J. Pstrus, *J. Electron. Mater.*, 31 (2002) 1.
- 7 G. P. Vassilev, E. S. Dobrev and J. C. Tedenac, *J. Alloys Compd.*, (2005) in publication.
- 8 http://www.ept.hut.fi/Research/Methods/Metallurgical_modelling.htm
- 9 Version 1.1 of the COST 531 Database for Lead Free Solders.
- 10 K. C. Chou, *Calphad*, 19 (1995) 315.

- 11 K. C. Chou, W. C. Li, F. Li and M. He, *Calphad.*, 20 (1996) 395.
- 12 G. W. Toop, *Trans. Met. Soc. AIME*, 233 (1965) 850.
- 13 M. Hillert, *Calphad*, 4 (1980) 1.
- 14 Y. M. Muggianu, M. Gambino and J. P. Bros, *J. Chim. Physique*, 72 (1975) 83.
- 15 F. Kohler, *Monatsh. Chem.*, 91 (1960) 738.
- 16 O. Redlich and A. T. Kister, *Ind. Eng. Chem.*, 24 (1948) 345.
- 17 Z. Moser, W. Gasior, J. Pstrus, W. Zakulski, I. Ohnuma, X. J. Liu, Y. Inohana and K. Ishida, *J. Electron. Mater.*, 30 (2001) 1120.
- 18 B. J. Lee, C. S. Oh and J. H. Shim, *J. Electron. Mater.*, 25 (1996) 983.
- 19 C. S. Oh, J. H. Shim, B. J. Lee and D. N. Lee, *J. Alloys Compd.*, 238 (1996) 155.
- 20 Pauling File Data Base: <http://crystdb.nims.go.jp>
- 21 F. Dan, M. H. Hamed and J. P. E. Grolier, *J. Therm. Anal. Cal.*, 85 (2006) 531.
- 22 M. A. A. O'Neill, S. Gaisford, A. E. Beezer, C. V. Skaria and P. Sears, *J. Therm. Anal. Cal.*, 84 (2006) 301.

Received: November 5, 2005

Accepted: December 28, 2006

OnlineFirst: April 29, 2007

DOI: 10.1007/s10973-005-7443-8